# REPORT 1022

## TEMPERATURE DISTRIBUTION IN INTERNALLY HEATED WALLS OF HEAT EXCHANGERS COMPOSED OF NONCIRCULAR FLOW PASSAGES[1]

By E. R. G. Eckert and George M. Low


### SUMMARY

*In the walls of heat exchangers composed of noncircular passages, the temperature varies in the circumferential direction because of local variations of the heat-transfer coefficients. A prediction of the magnitude of this variation is necessary in order to determine the region of highest temperature and in order to determine the admissible operating temperatures.*

*A method for the determination of these temperature distributions and of the heat-transfer characteristics of a special type of heat exchanger is developed. The heat exchanger is composed of polygonal flow passages and the passage walls are uniformly heated by internal heat sources. The coolant flow within the passages is assumed to be turbulent. The circumferential variation of the local heat-transfer coefficients is estimated from flow measurements made by Nikuradse, postulating similarity between velocity and temperature fields. Calculations of temperature distributions based on these heat-transfer coefficients are carried out and results for heat exchangers with triangular and rectangular passages are presented.*


### INTRODUCTION

The conventional recuperative type of heat exchanger consists of passages for two liquids or gases separated by a heating surface. Heat from an outside source is carried with a fluid flowing through one of the passages and is transferred in the heat exchanger to a second fluid flowing through the other passage. Very often such a heat exchanger is composed of a large number of tubes, with the two liquids flowing inside and over the outside of the tubes, respectively.

The regenerative type of heat exchanger has passages for one fluid only. During the heating period, heat from an outside source is carried to the heat exchanger by a hot fluid and is stored within the solid walls of the passages. This heat is then given off to a cold fluid, which passes through the heat exchanger during the cooling period.

In this report, a heat exchanger is considered that differs from the regenerative type only by the fact that the heat is generated by heat sources within the passage walls and is transferred to a coolant flowing continuously through the passages. The passage walls of this heat exchanger are assumed to be flat plates assembled to form a honeycomb; thus the flow passages formed in this manner have a polygonal cross section. A cross-sectional view of a typical heat exchanger of this type is shown in figure 1. The exchanger is composed of a number of plates $a$, which form the coolant passages $b$. The flow of the coolant is normal to the cross section shown. High temperatures may be anticipated near the corners $c$ of the passages, inasmuch as the rate of heat transfer there is expected to be poor. A theoretical investigation of the temperature distribution in such a heat exchanger was made at the NACA Lewis laboratory during 1950 and is presented herein.

The basis for this investigation is a knowledge of local heat-transfer coefficients in passages of noncircular cross section. Some information is available on the average heat-transfer coefficients in such tubes (references 1 and 2). The result of these investigations is essentially that the expressions derived for the heat-transfer coefficients in circular tubes apply for other cross sections as well, provided the diameter is replaced by the hydraulic diameter. (The hydraulic diameter is defined as four times the cross-sectional flow area divided by the circumference of the passage.)

A knowledge of local heat-transfer coefficients in noncircular passages is important not only in the present problem, but also for several other engineering problems, such as the determination of local temperatures in the walls of air-cooled turbine blades. No information on local heat-transfer coefficients was found in the available literature, however. These values are therefore estimated from flow measurements made by Nikuradse (reference 3) on the basis of the similarity between temperature and velocity fields.

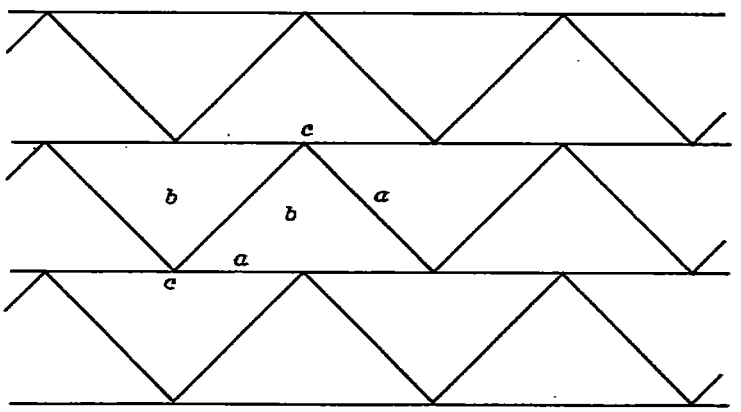


FIGURE 1.—Cross section through typical heat exchanger composed of noncircular flow passages.

[1] Supersedes NACA TN 2257, "Temperature Distribution in Internally Heated Walls of Heat Exchangers Composed of Noncircular Flow Passages" by E. R. G. Eckert and George M. Low, 1951.

## SYMBOLS

The following symbols are used in this report:

| | |
|---|---|
| $A$ | cross-sectional flow area (sq ft) |
| $A^*$ | ratio of wall area to flow area (dimensionless) |
| $C$ | internal circumference of passage (ft) |
| $C^*$ | $C/D$ (dimensionless) |
| $c_p$ | specific heat at constant pressure, Btu/(lb) (°F) |
| $D$ | hydraulic diameter, $4A/C$, (ft) |
| $g$ | acceleration due to gravity (ft)/(sec$^2$) |
| $h$ | local heat-transfer coefficient, Btu/(sec) (sq ft) (°F) |
| $\bar{h}$ | average heat-transfer coefficient, $\frac{1}{C}\int_0^C h\ dx$, Btu/(sec) (sq ft) (°F) |
| $h^*$ | $h/\bar{h}$ (dimensionless) |
| $k$ | thermal conductivity of wall material, Btu/(sec) (ft) (°F) |
| $k_g$ | thermal conductivity of coolant, Btu/(sec) (ft) (°F) |
| $k^*$ | $k/k_g$ (dimensionless) |
| $N$ | residual value (dimensionless) |
| $Nu$ | Nusselt number, $\bar{h}D/k_g$, (dimensionless) |
| $n$ | coordinate normal to passage wall (ft) |
| $n^*$ | $n/D$ (dimensionless) |
| $Pr$ | Prandtl number, $\nu/\alpha$, (dimensionless) |
| $p$ | pressure (lb)/(sq ft) |
| $q$ | local rate of heat transfer, $h\theta$, Btu/(sec) (sq ft) |
| $q^*$ | $h^*\ \theta^*$ (dimensionless) |
| $R$ | radial coordinate (ft) |
| $Re$ | Reynolds number, $uD/\nu$, (dimensionless) |
| $r$ | rate of internal heat generation, Btu/(sec) (cu ft) |
| $s$ | wall thickness (ft) |
| $s^*$ | $s/D$ (dimensionless) |
| $T$ | local total temperature of coolant, °F |
| $T_B$ | bulk total temperature of coolant, °F |
| $T^*$ | $Tk/rD^2$ (dimensionless) |
| $t$ | local wall temperature, °F |
| $t^*$ | $tk/rD^2$ (dimensionless) |
| $u, v$ | velocity components in $x$- and $y$-direction, respectively (ft/sec) |
| $x, y, z$ | Cartesian coordinates |
| $x^*$ | $x/D$ (dimensionless) |
| $y^*$ | $y/D$ (dimensionless) |
| $z^*$ | $z/D$ (dimensionless) |
| $\alpha$ | thermal diffusivity, $k_g/\rho g c_p$, (sq ft)/(sec) |
| $\beta$ | angle subtended by two adjacent sides of polygonal passage (deg) |
| $\Delta$ | increment of length (ft) |
| $\Delta^*$ | $\Delta/D$ (dimensionless) |
| $\delta$ | increment or difference |
| $\epsilon_H$ | turbulent diffusivity of heat (sq ft)/(sec) |
| $\epsilon_M$ | turbulent diffusivity of momentum (sq ft)/(sec) |
| $\theta$ | temperature difference, $t-T_B$, °F |
| $\theta^*$ | $\theta k/rD^2$ (dimensionless) |
| $\nu$ | kinematic viscosity (sq ft)/(sec) |
| $\rho$ | mass density (lb) (sec$^2$)/(ft$^4$) |
| $\tau_w$ | local wall shear stress (lb)/(sq ft) |

Subscripts:

| | |
|---|---|
| $c$ | conditions for equivalent circular tube |
| $m$ | conditions at center of flow passage |
| $n$ | conditions normal to passage wall |
| $s$ | conditions at wall surface |

Superscript:

| | |
|---|---|
| * | dimensionless quantity |

## ASSUMPTIONS

If this analysis were to be made without any simplifying assumptions, the simultaneous solution of the equations of motion of the coolant and of the heat flow in the coolant and in the passage walls would be required. The following assumptions are made in order to make these equations amenable to solution without seriously curtailing the results of the analysis:

(1) The Prandtl number of the coolant used in the heat exchanger is in the neighborhood of 1. This condition is well fulfilled by gases and by water above a temperature of 200° F, excluding the neighborhood of the critical point.

(2) The passages of the heat exchanger are long enough so that in the cross section investigated the flow is fully developed, which means that the velocity profile does not change its shape in the direction of the tube axis.

(3) The rate of heat generation in the walls of the heat exchanger is uniform. As a consequence of this condition, the temperature within the coolant and the walls increases linearly in a downstream direction provided the flow is thermally developed. For a fluid with a Prandtl number of 1, the points of thermal and velocity development in a tube practically coincide provided that the heating of the tube starts at the entrance section.

(4) The temperature gradient along the tube axis is assumed small as compared with the gradients in any cross section of the passage.

(5) The thermal conductivity of the solid material is large as compared with the thermal conductivity of the coolant. This condition is always fulfilled for metal walls regardless of the type of coolant used provided that assumption (1) applies and for nonmetallic walls if the coolant is a gas. For the case of nonmetallic walls and liquid coolants, the applicability of the calculations presented in this report must be checked in each individual case. Furthermore, the temperature differences within the passage wall at any one cross section are postulated to be small as compared with the temperature differences between the wall and the core of the coolant. As a consequence of the assumption listed in this paragraph, the heat transport within the coolant, normal to the tube axis and parallel to the walls, is small as compared with the heat conduction within the walls and may therefore be neglected. The heat transport within the coolant, normal to the tube axis and normal to the walls, is of course taken into account.

(6) The turbulent diffusivity of momentum $\epsilon_M$ and that of heat $\epsilon_H$ are equal.

## FLOW IN TUBES WITH NONCIRCULAR CROSS SECTION

A thorough investigation of the flow through tubes with noncircular cross sections was made by Nikuradse (reference 3). This investigation is used in the present report as the basis for estimating local heat-transfer coefficients.

The flow of water through tubes of several different shapes, as shown in figure 2, was investigated in reference 3. Three of the tubes had triangular cross sections; an equilateral triangle, an isosceles right triangle, and a right triangle with the sides enclosing the 90° angle having a ratio of 1 to 2.32. One tube had a trapezoidal cross section and two tubes were circular with one and two grooves, respectively. In a second report, Nikuradse investigated tubes with a rectangular cross section; however, only a summary of this report is available (reference 4). The hydraulic diameter of the passages varied from 0.3 to 0.6 inch and the length-to-hydraulic-diameter ratio varied from 100 to 200. The Reynolds number based on the hydraulic diameter and the mean velocity ranged from 77,000 to 120,000. Because it is known that the shape of a turbulent velocity profile changes only slightly with Reynolds number, the results of the calculations should be applicable for a fairly large range of Reynolds number in the turbulent region. The velocity profiles were measured with a small total-head tube in a cross section near the downstream end of the tube.

Results of reference 3 for the isosceles right triangle are shown in figures 3 to 5. Similar results for all other cross

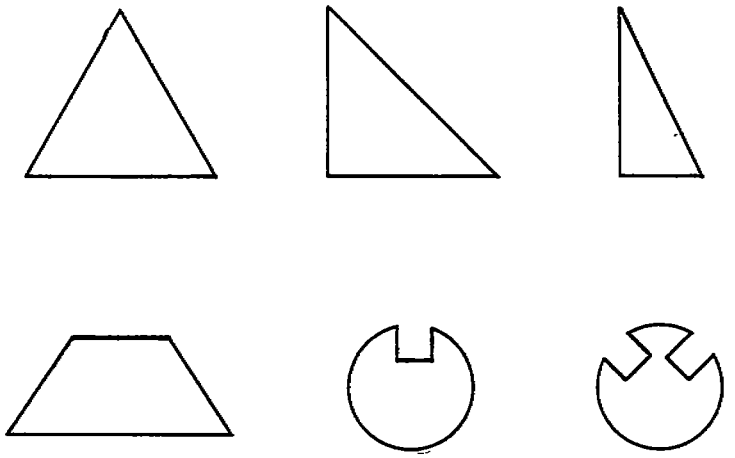

FIGURE 2.—Cross sections of passages investigated in reference 3.

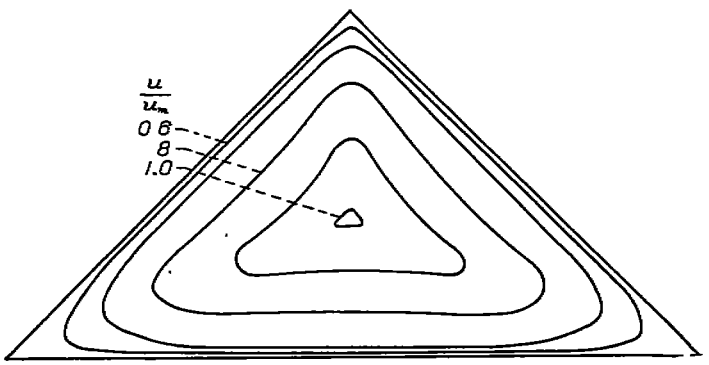


FIGURE 3.—Velocity contours in triangular passage as measured in reference 3. Reynolds number, 81,000.

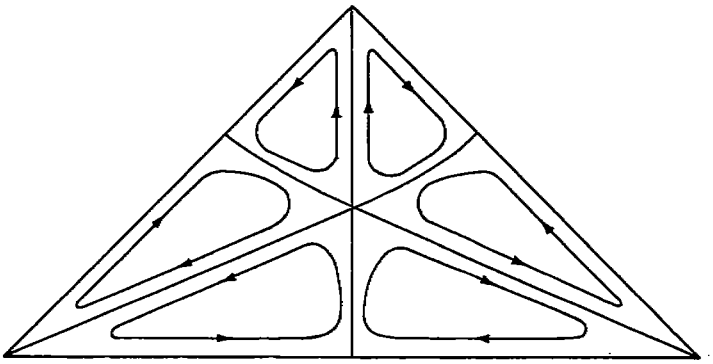

FIGURE 4.—Secondary flow in triangular passage deduced from measurements of reference 3.

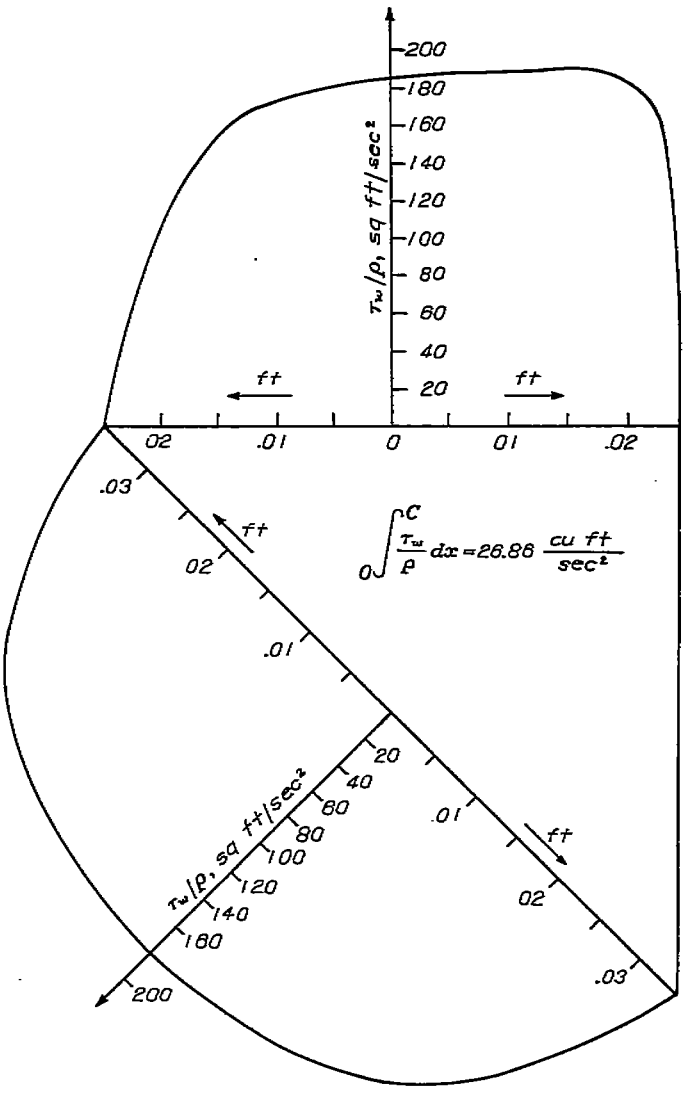


FIGURE 5.—Shear stress distribution on circumference of triangular passage as determined in reference 3.

sections can be found in the original report. In figure 3 the lines of constant velocity are presented as contour lines. These contours are indented near the center of each side of the passage. The conclusion of reference 3 is that these indentations indicate a secondary flow normal to the main flow direction. A qualitative sketch of this secondary flow is presented in figure 4. Prandtl (reference 5) has ascribed the secondary flow to a turbulent mixing motion within the fluid, which is more intense in the direction parallel to the wall than normal to it. This secondary flow tends to equalize the velocities and temperatures within any cross section of a noncircular tube and is therefore favorable for the similarity consideration that will be used to deduce the temperature field from the measured velocity field. On the other hand, because no quantitative knowledge of the secondary flow exists, an exact theoretical calculation of the temperature field in noncircular passages is impossible. The local wall shear stresses were computed by Nikuradse, using the measured velocity profiles together with the assumption that the Blasius pipe resistance law of the turbulent velocity profile for circular tubes applies also for noncircular passages on normals to the walls (fig. 5). A check by Nikuradse of the calculated average shear stresses against the measured pressure drop showed good agreement.

## SIMILARITY BETWEEN VELOCITY AND TEMPERATURE PROFILES FOR $Pr=1$

It is well known that the velocity and temperature profiles in the boundary layer of a fluid with a Prandtl number of 1 are similar in shape in the absence of a pressure gradient. This similarity is immediately apparent from a comparison of the momentum and energy equations of the boundary layer for two-dimensional steady flow along a flat plate (reference 6):

$$\rho\left(u\frac{\partial u}{\partial x}+v\frac{\partial u}{\partial y}\right)=\frac{\partial}{\partial y}\left[\rho(\nu+\epsilon_M)\frac{\partial u}{\partial y}\right] \tag{1}$$

$$\rho\left(u\frac{\partial T}{\partial x}+v\frac{\partial T}{\partial y}\right)=\frac{\partial}{\partial y}\left[\rho(\nu+\epsilon_H)\frac{\partial T}{\partial y}\right] \tag{2}$$

where $T$ represents the total temperature, the Prandtl number is equal to 1, and the specific heat is constant. The effect of internal friction on the temperature profile is taken into account by basing equation (2) on the total temperature.

Because it is assumed that the turbulent diffusivity of momentum $\epsilon_M$ and of heat $\epsilon_H$ are equal, equations (1) and (2) are similar. The solutions of the equations, namely, the velocity and temperature profiles, are therefore also similar, provided the boundary conditions are similar. The boundary conditions for the velocity field on a flat plate are that the velocity is 0 along the wall and has a constant value outside the boundary layer. Similar boundary conditions for the temperature field are that the temperature is constant both along the wall and in the main stream.

It is therefore evident that similarity between velocity and temperature profiles in the boundary layer over a flat plate exists in an exact mathematical sense. The same is not true, however, for fully developed pipe flow. The balance of the forces and of the heat energy on a stationary annular volume element with a radius $R$, thickness $dR$, and length (in the direction of the tube axis) $dz$, leads to the following equations for fully developed flow in a circular tube:

$$\frac{1}{R}\frac{\partial}{\partial R}\left[R\rho(\nu+\epsilon_M)\frac{\partial u}{\partial R}\right]=\frac{dp}{dz} \tag{3}$$

$$\frac{1}{R}\frac{\partial}{\partial R}\left[R\rho(\alpha+\epsilon_H)\frac{\partial T}{\partial R}\right]=\rho u\frac{\partial T}{\partial z} \tag{4}$$

where the heat-conduction term in the $z$-direction is neglected in equation (4). It is apparent that equations (3) and (4) are not similar, even if the viscosity and diffusivity terms in the two equations are equal. The following type of analysis can be made, however:

The turbulent diffusivity of momentum $\epsilon_M$ can be calculated from equation (3), provided that the velocity profile $u=f(R)$ and the pressure drop $dp/dz$ are experimentally known. If it is again assumed that $\epsilon_M$ and $\epsilon_H$ are equal, the temperature profile can then be calculated from equation (4). Such an analysis, based on constant property values and with internal friction neglected, was carried out by Latzko (reference 7). The results of this analysis were used to calculate the relation between the temperatures and the velocities for hydrodynamically and thermally developed flow of a fluid with $Pr=1$. Figure 6 represents a plot of the local temperature-difference ratio $(T-t_s)/(T_m-t_s)$ against the local velocity ratio $u/u_m$. It can be seen that this relation is very nearly linear. This linearity means that the velocity and temperature profiles are similar as far as practicality is con-

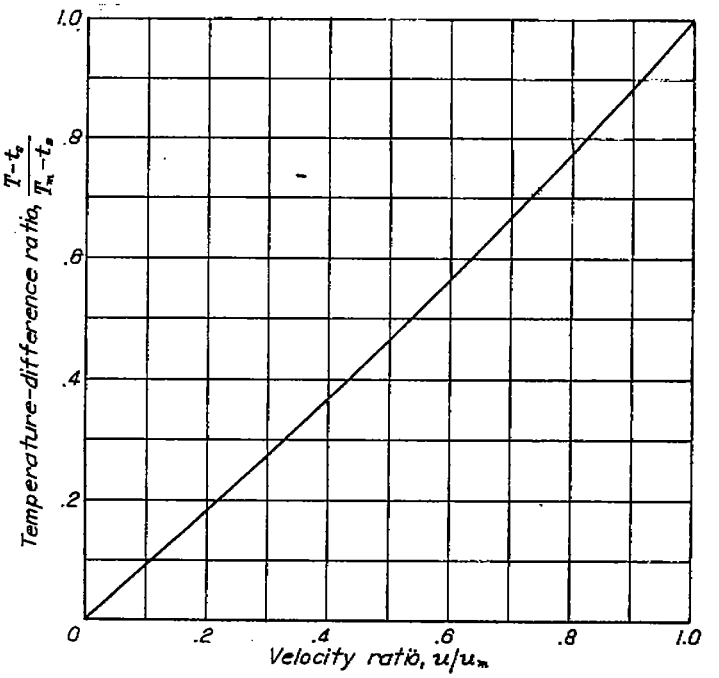


FIGURE 6.—Relation between local temperatures and local velocities in fully developed turbulent region of circular tube. Based on reference 7.

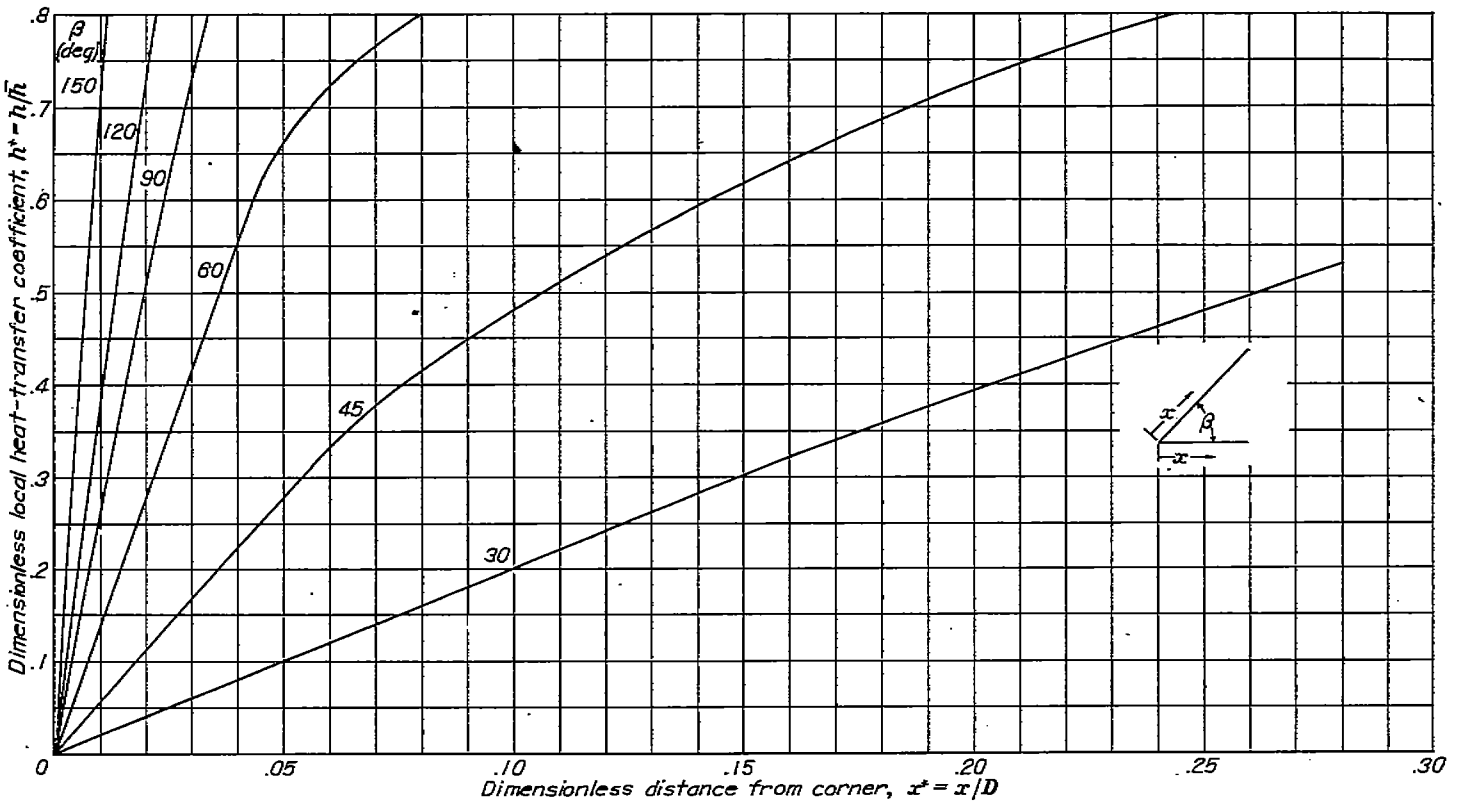


FIGURE 7. Local heat-transfer coefficients in corners of noncircular passages.

cerned, even though they are not similar in a strict mathematical sense. Most of the recent theoretical investigations of turbulent heat transfer are therefore based on the assumption of similarity between these profiles for a fluid with a Prandtl number of 1.

It is known that the fully developed turbulent velocity profile in a circular tube is such that the essential part of the velocity change from 0 at the wall to a maximum value at the center occurs in a narrow strip around the periphery of the tube. The investigations of references 3 and 4 show that this condition is also true for tubes of polygonal cross section, as long as the included angles between two adjacent passage walls are not very small. Nikuradse further shows that the law for the velocity variation on a normal to the wall established for turbulent flow in circular tubes holds also for the noncircular passages in this region of essential velocity variation. It can therefore be expected that the similarity between temperature and velocity profiles will also be fulfilled reasonably well on normals to the walls for noncircular tubes and fluids with a Prandtl number of 1, although a balance of forces and energies similar to equations (3) and (4) shows that the similarity cannot exist exactly in regions very close to the corners.

An immediate result of the similarity between velocity and temperature profiles is the fact that the local wall shear stress determined by the velocity gradient at the wall is proportional to the local heat-transfer coefficient determined by the temperature gradient at the wall. (The same result can be obtained from Reynolds' analogy.) The proportionality of these values, together with the knowledge that the average heat-transfer coefficients for circular and noncircular tubes with the same hydraulic diameter are equal, can be used to obtain local heat-transfer coefficients in noncircular tubes from the wall-shear-stress data of references 3 and 4. A generalization of this result is possible because, for a given Reynolds number, the shear stress distribution in the vicinity of a corner of the passage depends primarily on the conditions near that corner and not on the shape of the passage.

The local heat-transfer coefficients, as presented in figure 7, were obtained by correlating the results of references 3 and 4. In this figure the ratio $h^*$ of the local heat-transfer coefficient to the mean value is plotted against the dimensionless distance from the corner $x^*$. The included angle of two adjacent passage walls is the parameter for the curves. Some of these corner angles were represented on more than one of the cross sections investigated in reference 3, and for these angles the curves of $h^*$ against $x^*$ agree reasonably well.

The application of figure 7 can best be explained with the aid of an example. Suppose it is desired to find the distribution of $h^*$ over the short leg of an isosceles right triangle, as shown in figure 8. The two ends of the curve can immediately be transposed from figure 7. The remainder of the curve is then extrapolated so that the area under the curve divided by length $\overline{AB}$ is equal to 1. This procedure gives a reasonably good approximation as long as the maximum value of $h^*$ is not considerably greater than 1.

## DIMENSIONLESS VARIABLES

With the distribution of the local heat-transfer coefficient around the circumference of the passages established, the only problem remaining to be solved is the calculation of the heat-conduction process within the passage walls. Before this problem is taken up, an investigation is made to determine the dimensionless moduli on which the temperature distribution in a heat exchanger of the type under consideration depends. This investigation may be useful as a basis for experimental investigations. None of the simplifying assumptions, as summarized previously, is necessary for the development in this section of the report.

The heat conduction within the solid walls of a heat exchanger with internal heat generation is described by Poisson's equation

$$k\left(\frac{\partial^2 t}{\partial x^2}+\frac{\partial^2 t}{\partial y^2}+\frac{\partial^2 t}{\partial z^2}\right)+r=0 \tag{5}$$

The number of parameters for this equation can be reduced by the use of the following dimensionless values:

$$t^*=\frac{tk}{rD^2} \qquad x^*=\frac{x}{D} \qquad y^*=\frac{y}{D} \qquad z^*=\frac{z}{D} \tag{6}$$

With these values, equation (5) can be rewritten

$$\frac{\partial^2 t^*}{\partial x^{*2}}+\frac{\partial^2 t^*}{\partial y^{*2}}+\frac{\partial^2 t^*}{\partial z^{*2}}+1=0 \tag{7}$$

The temperature field that results under the influence of the internal heat generation in the solid walls depends on how the heat is transferred from the wall surfaces to the coolant. The heat must be conducted within the solid material to the surface and from there into the coolant. Along the surface, therefore, the following boundary condition exists:

$$k\left(\frac{\partial t}{\partial n}\right)_s=k_g\left(\frac{\partial T}{\partial n}\right)_s \tag{8}$$

where $n$ represents the direction normal to the surface. In terms of dimensionless variables, this equation becomes

$$k^*\left(\frac{\partial t^*}{\partial n^*}\right)_s=\left(\frac{\partial T^*}{\partial n^*}\right)_s \tag{9}$$

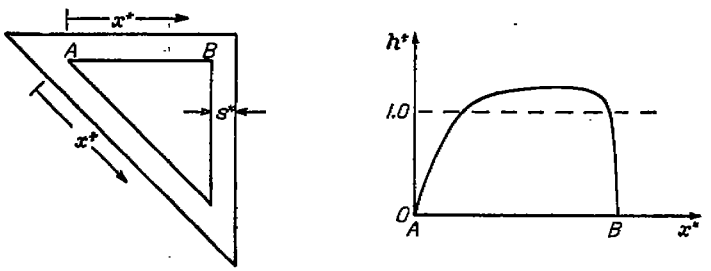


FIGURE 8.—Determination of local heat-transfer coefficients in triangular heat-exchanger passage.

The heat transfer within the coolant by conduction and convection is governed by an energy equation similar to equation (4) and the flow of the coolant is determined by a momentum equation (similar to equation (3)) and the corresponding continuity equation. Textbooks on heat transfer (for example, reference 8) show that the dimensionless temperature described by the energy equation of the coolant depends, for low-velocity flow and constant property values, on the Reynolds number $Re$ and the Prandtl number $Pr$. At high velocities and variable property values, there is an additional influence of the Mach number and other dimensionless expressions characterizing the temperature dependency on the property values. By neglecting the last-mentioned influences and summarizing all the factors that influence the heat flow in the solid material and in the coolant, a functional relation of the following type can be deduced:

$$\theta^*=f(Re,\ Pr,\ k^*,\ x^*,\ y^*,\ z^*) \tag{10}$$

where the temperature difference $\theta^*$ is introduced because only temperature differentials appear in the equations. The function $f$ as expressed by this equation depends on the geometric configuration of the heat-exchanger passages.

When it can be assumed that the heat-transfer process from the walls to the coolant is not influenced by the temperature distribution within the wall, the number of factors influencing the problem can be considerably reduced. This assumption is made throughout the calculations in this report and seems reasonable as long as previously mentioned assumption (5) holds. In this case equation (8) can be replaced by

$$k\left(\frac{\partial t}{\partial n}\right)_s=-h(t_s-T_B) \tag{11}$$

where $h$ is a known function of the flow parameters. By introducing the ratio $h^*$ of the local heat-transfer coefficient to the value averaged over the circumference of the passage and the Nusselt number $Nu=\bar{h}D/k_g$ based on this average value, and by changing to the temperature difference $\theta$, equation (11) can be transformed to

$$\left(\frac{\partial \theta^*}{\partial n^*}\right)_s=-Nu\frac{h^*}{k^*}\theta_s^* \tag{12}$$

The dimensionless temperature within the solid walls of the heat exchanger is determined by equations (7) and (12) and can be presented as a function of the following kind:

$$\theta^*=f\left(Nu\frac{h^*}{k^*},\ x^*,\ y^*,\ z^*\right) \tag{13}$$

This dimensionless temperature difference depends only on the dimensionless local coordinates and on the parameter $Nu\frac{h^*}{k^*}$. Temperature distributions and heat-transfer characteristics for any given geometric configuration are therefore presented as a one-parameter family of curves.

## CALCULATION OF TEMPERATURE DISTRIBUTIONS WITHIN PASSAGE WALLS

The problem of calculating temperature distributions within the passage walls can be classified in two general categories, depending on the relative thickness of these walls. If the dimensionless wall thickness $s^*$ (see fig. 8) is small as compared with the length of a wall $\overline{AB}$, the temperature differences in the direction normal to the wall surface are small as compared with the temperature difference in the direction $x^*$ parallel to the surface. Only the temperature differences in this parallel direction need therefore be considered. Hereinafter this special case of the problem is referred to as the "one-dimensional problem." On the other hand, if $s^*$ becomes large, the heat flow in both the $x^*$ and $s^*$ directions must be considered. This second and more general problem is referred to as the "two-dimensional problem."

**One-dimensional problem.**—Consider a thin plate of thickness $s$ that is a section of the heat-exchanger passage walls. Heat is generated uniformly throughout the plate at a rate $r$. The local plate (or wall) temperature $t$ is assumed to be varying in the $x$-direction only. The bulk temperature of the coolant is $T_B$ and the thermal conductivities of the wall and coolant are $k$ and $k_g$, respectively. The local coefficients of heat transfer to the coolant above and below the plate are denoted by $h$ and $h'$, as shown in the following sketch:

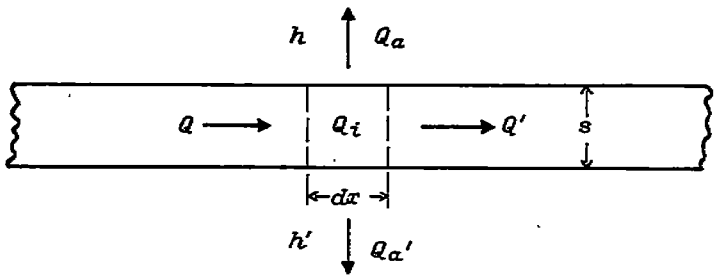


The heat balance for an element of volume with the dimensions $dx$ and $s$ and of unit depth is

$$Q+Q_i=Q'+Q_a+Q_a' \tag{14}$$

where

$$Q=-ks\frac{dt}{dx}$$

$$Q'=-ks\left(\frac{dt}{dx}+\frac{d^2t}{dx^2}dx\right)$$

$$Q_i=rs\,dx$$

$$Q_a+Q_a'=(h+h')(t-T_B)\,dx$$

With the preceding values of $Q$, equation (14) becomes

$$\frac{d^2t}{dx^2}-\frac{h+h'}{ks}(t-T_B)+\frac{r}{k}=0 \tag{15}$$

Equation (15) can be expressed in terms of dimensionless variables as

$$\frac{d^2\theta^*}{dx^{*2}}-\frac{h^*+h'^*}{s^*k^*}Nu\,\theta^*+1=0 \tag{16}$$

This equation expresses the dimensionless wall temperature $\theta^*$ as a function of the dimensionless coordinate $x^*$ and a single parameter $(h^*+h'^*)Nu/s^*k^*$. For any given geometric configuration (which determines $h^*$ and $h'^*$ as functions of $x^*$), the dimensionless wall temperature is a function only of the average Nusselt number $Nu$, the dimensionless wall thickness $s^*$, and the ratio of the thermal conductivities $k^*$.

In general, equation (16) must be solved by numerical means inasmuch as $h^*$ and $h'^*$ are experimentally determined functions of $x^*$. Several numerical methods of solution can be applied and two of these are considered here. The relaxation method (see, for example, reference 2, pp. 365–379, or reference 9) has the advantage that it is easy to apply and that computational errors are immediately apparent. A second method of solution, based on the Runge-Kutta method (reference 10) is presented in the appendix. This method is preferable when results of high accuracy are desired. It is less convenient, however, than the relaxation method because computational errors are much more difficult to detect.

For the purpose of solving equation (16) by the relaxation method, the equation is first expressed in finite-difference form. Consider a grid, or net of points, placed into the wall, any two adjacent points being separated by a small but finite distance $\Delta^*$, as indicated in the following sketch:

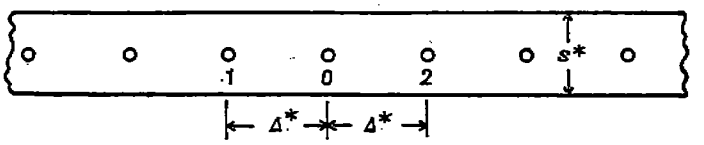


The second derivative of $\theta^*$ at an arbitrary point 0 can be expressed in terms of the temperatures $\theta^*$ at this point and the two adjacent points as follows:

$$\left(\frac{d\theta^*}{dx^*}\right)_0\approx\frac{\theta_1^*-\theta_0^*}{\Delta^*} \qquad \left(\frac{d\theta^*}{dx^*}\right)_2\approx\frac{\theta_0^*-\theta_2^*}{\Delta^*}$$

$$\frac{d^2\theta^*}{dx^{*2}}\approx\frac{1}{\Delta^*}\left[\left(\frac{d\theta^*}{dx^*}\right)_1-\left(\frac{d\theta^*}{dx^*}\right)_2\right]$$

$$\approx\frac{1}{\Delta^{*2}}(\theta_1^*+\theta_2^*-2\theta_0^*) \tag{17}$$

With this value for the second derivative, equation (16) becomes

$$\theta_1^*+\theta_2^*-\theta_0^*\left[2+\frac{Nu}{s^*k^*}(h^*+h'^*)_0\Delta^{*2}\right]+\Delta^{*2}=0 \tag{18}$$

The relaxation method, used for solving this equation, is subsequently discussed.

**Two-dimensional problem.**—Consider a slab of homogeneous solid material with unit thickness, as shown in the following diagram:

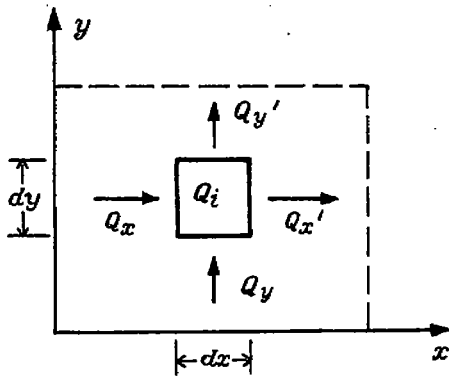


Heat is again generated within the material at a uniform rate $r$. The heat balance for an element of volume with the dimensions $dx$ and $dy$ and of unit depth is

$$Q_x+Q_y+Q_i=Q_x'+Q_y' \tag{19}$$

A constant flow of heat through the slab normal to the plane of the preceding sketch does not influence this heat balance. Local deviations from this constant flow of heat are neglected.

The individual terms in equation (19) are

$$Q_x=-k\,dy\frac{\partial t}{\partial x}$$

$$Q_x'=-k\,dy\left(\frac{\partial t}{\partial x}+\frac{\partial^2 t}{\partial x^2}dx\right)$$

$$Q_y=-k\,dx\frac{\partial t}{\partial y}$$

$$Q_y'=-k\,dx\left(\frac{\partial t}{\partial y}+\frac{\partial^2 t}{\partial y^2}dy\right)$$

$$Q_i=r\,dx\,dy$$

Equation (19) can therefore be written

$$\frac{\partial^2 t}{\partial x^2}+\frac{\partial^2 t}{\partial y^2}=-\frac{r}{k} \tag{20}$$

Or, in terms of the dimensionless variables,

$$\frac{\partial^2\theta^*}{\partial x^{*2}}+\frac{\partial^2\theta^*}{\partial y^{*2}}=-1 \tag{21}$$

If the slab is bounded by a coolant whose bulk temperature is $T_B$ and if the local surface heat-transfer coefficient at a point $s$ on the surface is $h$, the boundary condition at that point is

$$k\left(\frac{\partial t}{\partial n}\right)_s=-h(t-T_B)_s \tag{22}$$

where $n$ is the direction normal to the surface. Equation (22) can again be written in terms of the dimensionless variables

$$\left(\frac{\partial\theta^*}{\partial n^*}\right)_s=-\frac{Nu\,h^*}{k^*}\theta_s^* \tag{23}$$

Equation (21) together with boundary condition (23) fully describes the two-dimensional problem. All physical variables are again grouped into a single parameter $h^*\,Nu/k^*$, which appears in the boundary condition. In order to apply the relaxation method of solution to these expressions, they are first converted to difference equations.

For this purpose a rectangular grid is placed into the slab, as indicated in the following diagram:

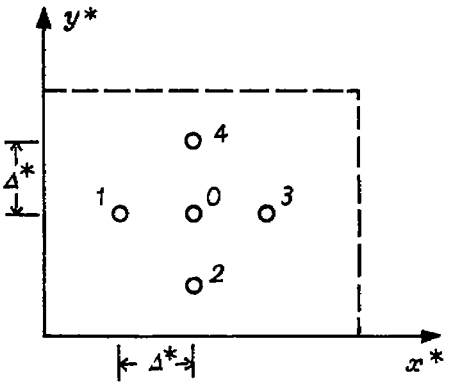


Adjacent net points are separated by a distance $\Delta^*$. The derivatives of $\theta^*$ at an arbitrary point 0 can be expressed in terms of the temperature function at surrounding points. Thus the first derivatives are

$${}_1\left(\frac{\partial\theta^*}{\partial x^*}\right)_0\approx\frac{\theta_1^*-\theta_0^*}{\Delta^*} \qquad {}_0\left(\frac{\partial\theta^*}{\partial x^*}\right)_3\approx\frac{\theta_0^*-\theta_3^*}{\Delta^*}$$

$${}_2\left(\frac{\partial\theta^*}{\partial y^*}\right)_0\approx\frac{\theta_2^*-\theta_0^*}{\Delta^*} \qquad {}_0\left(\frac{\partial\theta^*}{\partial y^*}\right)_4\approx\frac{\theta_0^*-\theta_4^*}{\Delta^*}$$

and the second derivatives become

$$\frac{\partial^2\theta^*}{\partial x^{*2}}\approx\frac{\theta_1^*+\theta_3^*-2\theta_0^*}{\Delta^{*2}}$$

$$\frac{\partial^2\theta^*}{\partial y^{*2}}\approx\frac{\theta_2^*+\theta_4^*-2\theta_0^*}{\Delta^{*2}}$$

With these values, equation (21) becomes

$$\theta_1^*+\theta_2^*+\theta_3^*+\theta_4^*-4\theta_0^*+\Delta^{*2}=0 \tag{24}$$

The boundary condition can be evaluated by assuming that points 1, 0, and 3 lie on the surface of the wall. Point 4 then lies in the stream and its temperature must be expressed by the normal derivative at point 0.

$${}_4\left(\frac{\partial\theta^*}{\partial y^*}\right)_0\approx\frac{\theta_4^*-\theta_0^*}{\Delta^*}$$

or, with the use of the value of $\partial\theta^*/\partial y^*$ as given by equation (23),

$$\theta_4^*=\theta_0^*\left(1-\frac{Nu\,h^*}{k^*}\Delta^*\right) \tag{25}$$

Along the boundary, therefore, the following equation applies:

$$\theta_1^*+\theta_2^*+\theta_3^*-\theta_0^*\left(3+\frac{Nu\,h^*}{k^*}\Delta^*\right)+\Delta^{*2}=0 \tag{26}$$

Equation (24) together with boundary condition (26) can again be solved by means of the relaxation method.

Solution by relaxation method.—A heat exchanger composed of a large number of rectangular passages will be discussed. The walls of the heat exchanger are made of a homogeneous material in which heat is generated at a uniform rate $r$. Figure 9 represents a cut through the heat exchanger so that the flow of coolant is in a direction normal to the cut. In the discussion that follows, it is assumed that the geometry of the configuration is given in the dimensionless system of coordinates.

A complete discussion of the relaxation method is not presented herein, inasmuch as it is generally available elsewhere. (See, for example, reference 9.) The essential features of the method can be outlined as follows:

Suppose it is desired to solve a given finite-difference equation over a certain area of integration. The equation is of the following type:

$$f(\theta^*)=0 \tag{29}$$

The solution of equation (29) must also satisfy prescribed conditions at the boundary of the area of integration.

First, it is necessary to select a number of net points covering the entire area of integration. The distance $\Delta^*$ between net points is arbitrary, with the accuracy of the final solution increasing as the distance between points is decreased. Next, values of $\theta^*$ are assumed at each net point. If by chance these assumed values of $\theta^*$ are the correct values, then they satisfy the appropriate finite-difference equation at all net points.

In general, however, the assumed values of the function do not satisfy the difference equation and the left side of equation (29) is equal to some residual value $N$ instead of zero. At any given net point $\theta^*$ must then be adjusted in order to make $N$ vanish at that point. This adjustment of $\theta^*$ also changes the residuals at adjacent net points. However, if this process of adjustment is started at the point at which the absolute value of $N$ is greatest and is then repeated for points at which the value of the residual is successively less, the correct values of $\theta^*$ for the entire net eventually are obtained.

In applying this method to the heat exchanger under consideration, it is first assumed that the wall thickness $s^*$ is small, so that the one-dimensional solution applies.

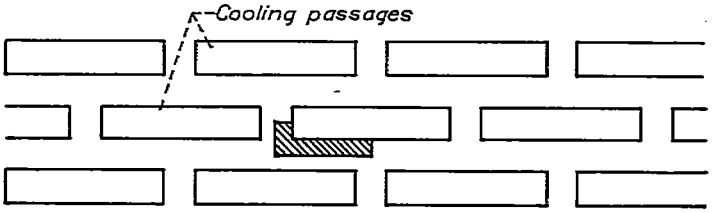


FIGURE 9.—Thick-walled heat exchanger with rectangular passages. (Shaded region is considered in calculations.)

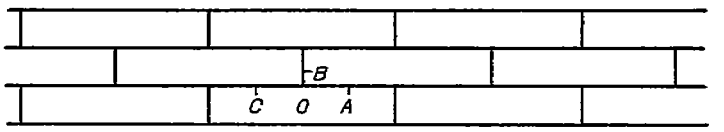


FIGURE 10.—Thin-walled heat exchanger with rectangular passages. (Calculation is confined to region ABC.)

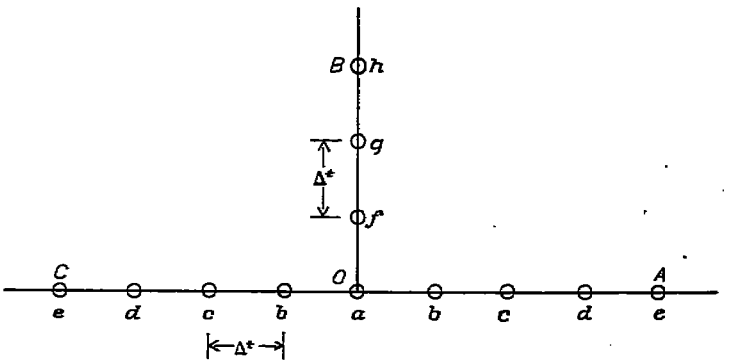


FIGURE 11.—Relaxation net for rectangular thin-walled heat exchanger.

The actual configuration to be discussed is shown in figure 10. Because points A, B, and C are points of symmetry, only the region bounded by these points need be considered. Furthermore, the distribution of temperature is also symmetric about point O with respect to AO and OC. An enlarged view of the section under consideration is represented in figure 11.

The section has been subdivided into a number of net points $a, b, c, \ldots h$, each separated by a distance $\Delta^*$ from adjacent points. The first step in the analysis is the assumption of temperatures at all net points, which can be done by setting up a balance between the total heat produced within the walls and the total outflow of heat from the walls. In terms of the dimensionless variables, this heat balance becomes

$$\frac{1}{C^*}\frac{Nu}{k^*s^*}\int_0^{C^*}\theta^*(h^*+h'^*)\,dx^*=1 \tag{30}$$

If, for the initial assumption, $h^*=h'^*=1$ and $\theta^*$ is constant, the following expression is obtained:

$$\theta^*=\frac{s^*k^*}{2Nu} \tag{31}$$

The value of $\theta^*$ given by equation (31) is assumed to exist at all net points. The appropriate difference equation at points $b, c, d, f$, and $g$ is (from equation (18))

$$\theta_1^*+\theta_2^*-\theta_0^*\left[2+\frac{Nu}{s^*k^*}(h^*+h'^*)_0\Delta^{*2}\right]+\Delta^{*2}=N_0 \quad (32)$$

where the subscript 0 refers to the point at which the equation is to be applied and subscripts 1 and 2 refer to adjacent points. At point $a$, which is influenced by three points, the following equation is required:

$$2\theta_b^*+\theta_f^*-\theta_a^*\left[3+\frac{Nu}{s^*k^*}(h^*+h'^*)_a\Delta^{*2}\right]+\Delta^{*2}=N_a \quad (33)$$

At point $e$, which is a point of symmetry, the following expression applies:

$$2\theta_d^*-\theta_e^*\left[2+\frac{Nu}{s^*k^*}(h^*+h'^*)_e\Delta^{*2}\right]+\Delta^{*2}=N_e \quad (34)$$

A similar expression applies at point $h$. With these equations, the residuals $N$ are calculated at each net point. The point at which $N$ has the largest absolute value is then selected and $\theta^*$ at that point is adjusted so that the residual vanishes. The effect of this adjustment on the residuals at adjacent points is calculated with the aid of the appropriate finite-difference equation.

The process is repeated for the point at which the next largest value of the residual appears. Eventually, if the process is repeated often enough, the residuals at all net points approach zero. The final adjusted values of $\theta^*$ then satisfy the appropriate equations at all net points.

These values of $\theta^*$ should also satisfy the heat balance as given by equation (30). This equation can therefore be used to check the validity of the final temperature distribution. If the check is unsatisfactory, it is necessary to continue the solution of the finite-difference equations by using a smaller net spacing.

The same heat-exchanger configuration is now investigated without making the assumption that the wall thickness is small. The two-dimensional equations are therefore applied. An enlarged view of the shaded portion of figure 9 is shown in figure 12. The lines $\overline{CD}$, $\overline{FG}$, and $\overline{GA}$ are lines of symmetry, and there is no flow of heat across these lines. The temperature distribution along line $\overline{DEF}$ will be symmetric about point E, but there will be a flow of heat across this line. A large number of net points are selected to cover the entire section of the configuration shown in figure 12. (Only a few of these points are presented in the fig.) An initial value for the temperature along lines $\overline{AB}$ and $\overline{BC}$ is obtained by setting up a balance between the total heat produced within the section and the flow of heat to the gas. In terms of the dimensionless variables, this heat balance becomes

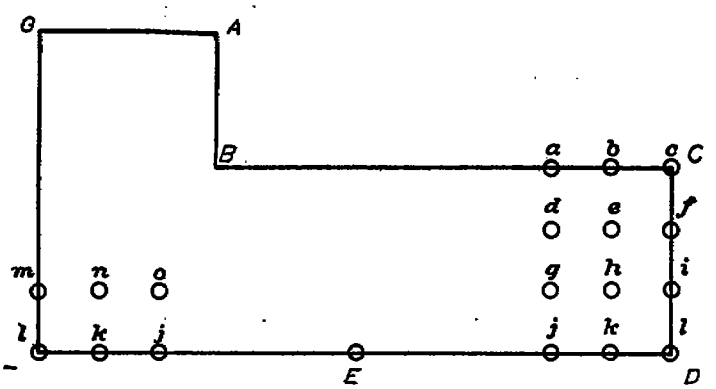


FIGURE 12.—Relaxation net for rectangular thick-walled heat exchanger.

$$\frac{1}{C^*}\int_0^{C^*}h^*\theta^*\,dx^*=\frac{A^*}{4}\frac{k^*}{Nu} \quad (35)$$

If, for the initial assumption, $h^*=1$ and $\theta^*$ is constant, then the following expression for $\theta^*$ is obtained:

$$\theta^*=\frac{A^*}{4}\frac{k^*}{Nu} \quad (36)$$

It can now be assumed that the temperature as given by equation (36) exists along the surface of the wall and that a somewhat higher temperature exists at internal points. The assumed temperatures are then adjusted by means of the relaxation method.

The appropriate finite-difference equation for internal points, such as point $e$, is written as follows:

$$\theta_b^*+\theta_f^*+\theta_h^*+\theta_d^*-4\theta_e+\Delta^{*2}=N_e \quad (37)$$

For points along the boundary, such as point $b$, the equation is

$$\theta_a^*+\theta_e^*+\theta_c^*-\theta_b^*\left(3+\frac{Nu}{k^*}h_b^*\Delta^*\right)+\Delta^{*2}=N_b \quad (38)$$

and for points on a line of symmetry, such as point $f$,

$$\theta_c^*+2\theta_e^*+\theta_i^*-4\theta_f^*+\Delta^{*2}=N_f \quad (39)$$

The appropriate equation for points along $\overline{DEF}$ can be determined by taking advantage of the antisymmetry about this line. At point $k$, for instance, the equation becomes

$$\theta_h^*+\theta_l^*+\theta_n^*+\theta_j^*-4\theta_k^*+\Delta^{*2}=N_k \quad (40)$$

Expressions of the type (37) to (40) apply at all net points. The method of determining the actual temperature distribution is the same as the method outlined in the previous section.

The final temperatures along the surface of the wall can be checked with the aid of equation (35). If the check is unsatisfactory, a finer net spacing is required.

## RESULTS

**One-dimensional solution.**—The one-dimensional solution was applied to heat exchangers composed of rectangular and triangular passages, respectively. In each case the passages were staggered in order to minimize the expected hot spots.

The rectangular configuration is represented by figure 10. The height-to-width ratio of each passage in this configuration is 1 to 5. Figure 1 represents the triangular configuration. Each passage in this configuration is an isosceles right triangle.

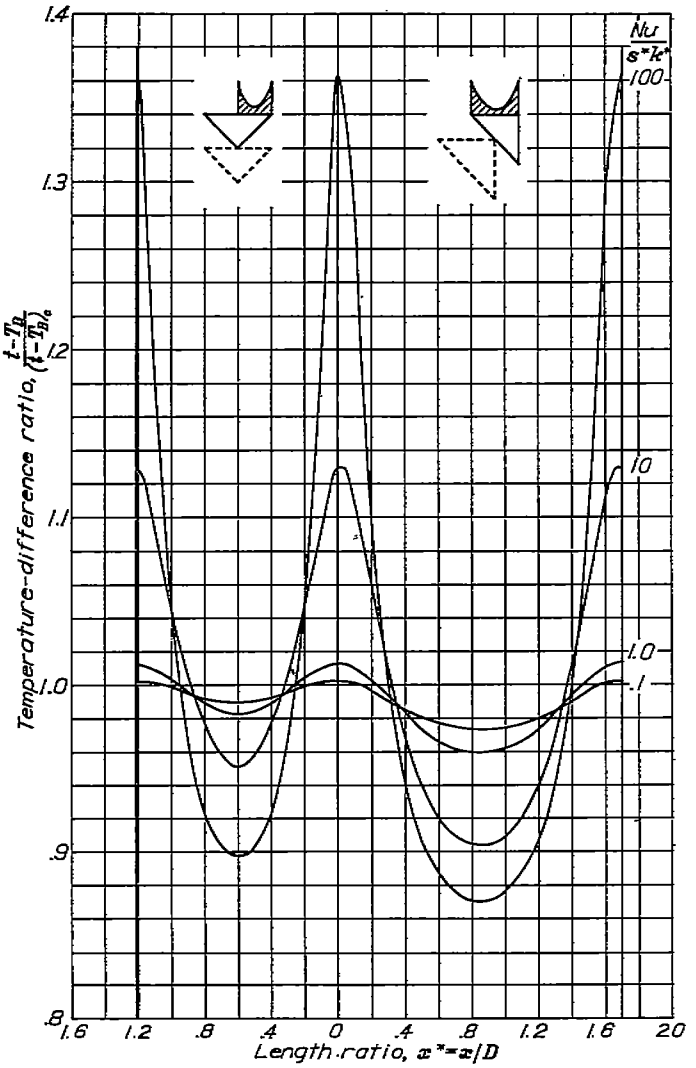


FIGURE 13.—Temperature distribution for passage of thin-walled triangular heat exchanger (fig. 1).

It has previously been stated that, for each configuration, the temperature distribution in the passage walls is a function only of the parameter $Nu/s^*k^*$. Accordingly, temperature distributions were calculated for several values of this parameter, ranging from 0.1 to 100. This range of values is believed to include all values actually encountered.

Temperature distributions were calculated according to the method outlined in the previous section of this report and were then checked by equation (30). Local rates of heat transfer $q^* \equiv h^*\theta^*$ were calculated for this purpose. According to equation (30), the mean value of $q^*$ when multiplied by $2Nu/k^*s^*$ should equal 1. Because the finite-difference method of solution is essentially an approximate method, the results were not expected to be exact. All results presented in this section of the report, however, were held to an error of less than 6 percent. The final temperatures were multiplied by a constant scale factor in order to satisfy equation (30) exactly.

Temperature distributions and local rates of heat transfer are presented for the triangular heat exchanger in figures 13 and 14 and for the rectangular heat exchanger in figures 15 and 16. In the temperature plots (figs. 13 and 15), the temperature difference $(t-T_B)$ is referred to the temperature difference $(t-T_B)_c$ for a thin-walled circular tube with the same hydraulic diameter and an internally heated wall with the same physical properties. The temperature difference for the circular tube is given in the nondimensional form by equation (31). Similarly, the ordinate in figures 14 and 16 refers the rate of heat transfer $q$ to the rate of heat transfer from the wall of a thin circular tube $q_c$. It is believed that

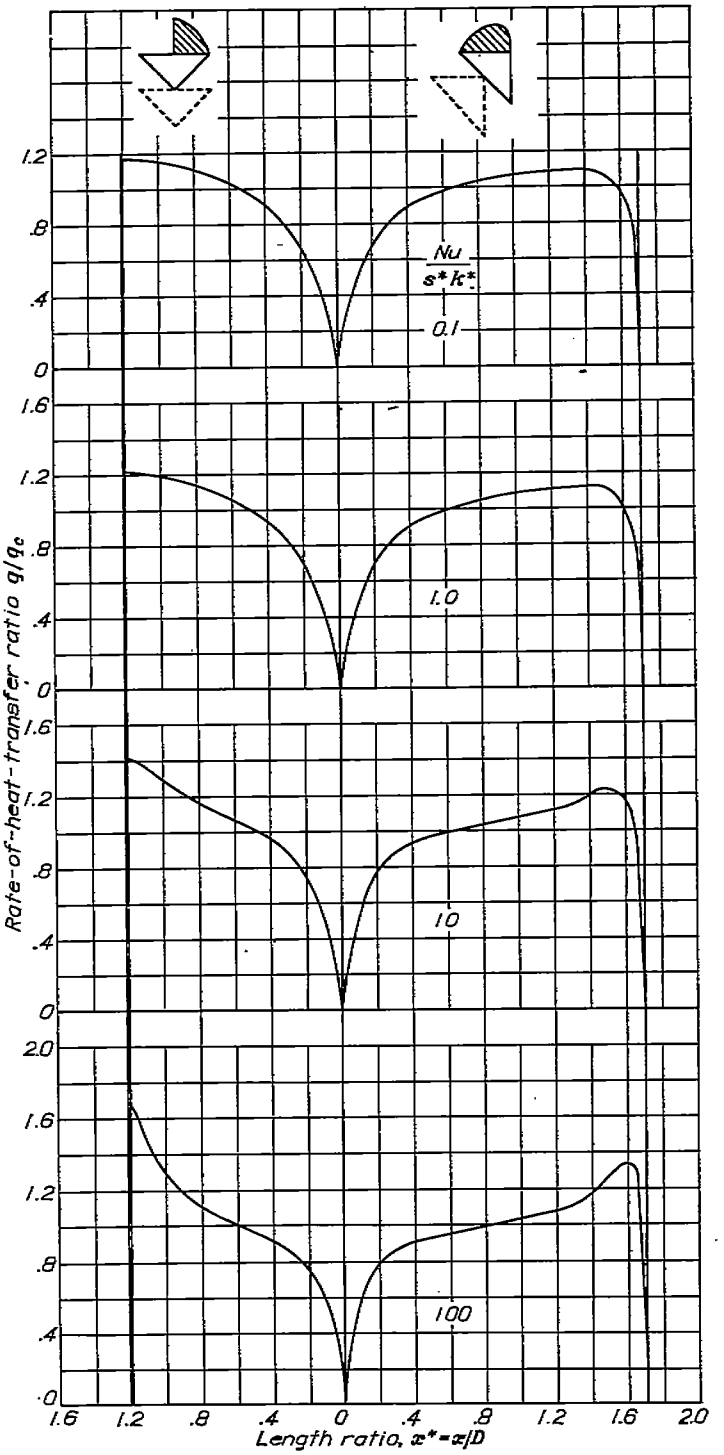


FIGURE 14.—Local rate of heat transfer from passage of thin-walled heat exchanger (fig. 1).

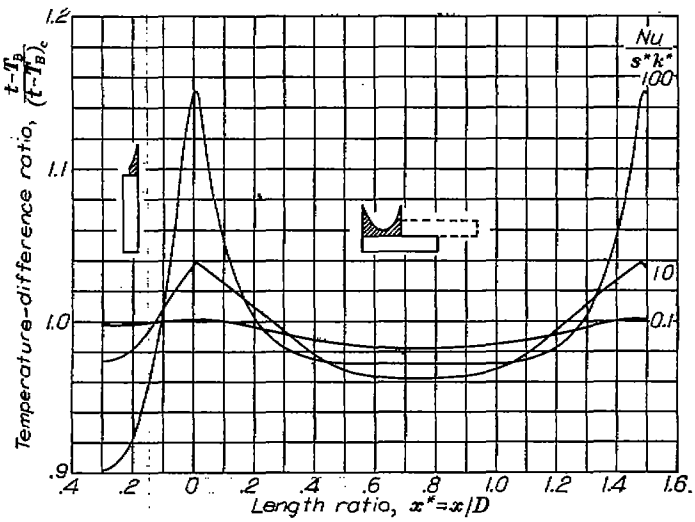


FIGURE 15.—Temperature distribution for passage of thin-walled rectangular heat exchanger (fig. 10).

the interpretation of the temperature and heat-transfer curves is simplified by this final change of ordinates. Temperature distributions for the triangular configuration are shown in figure 13. These curves are presented for values of $Nu/s^*k^*$ of 0.1, 1.0, 10, and 100. As was expected, the temperatures peak near the corners of the passage. The largest temperature differences are encountered for large values of the parameter $Nu/s^*k^*$. A large value of this parameter indicates a low conductivity of the wall material or a small wall thickness. Both of these conditions are conducive to low rates of heat exchange within the wall. Local rates of heat transfer corresponding to the temperature distributions just discussed are presented in figure 14.

Temperature and heat-transfer curves for the rectangular configuration are shown in figures 15 and 16. The results for this configuration are similar to those for the triangular configuration.

In order to determine when the one-dimensional solution can be used, it is necessary to obtain some information on the temperature difference that exists across the passage walls on normals to the surfaces and to compare this temperature difference with the temperature differences along the surfaces. An estimate of the temperature difference $\delta t_n$ across the wall may be obtained by calculating this value for a flat plate. The result of this calculation is

$$\delta t_n = \frac{r}{8k} s^2 \tag{41}$$

The equation can be changed to the dimensionless values to yield

$$\delta t_n{}^* = \frac{s^{*2}}{8} \tag{42}$$

This temperature difference can again be referred to the temperature difference $(t-T_B)_c$ as follows:

$$\frac{\delta t_n}{(t-T_B)_c} = \frac{s^* Nu}{4k^*} \tag{43}$$

The one-dimensional solution applies as long as this value is small as compared with the temperature differences presented in figures 13 and 15.

**Two-dimensional solution.**—The two-dimensional solution for the temperature field within the heat exchanger depends on two parameters; namely, the dimensionless wall thickness $s^*$ and the value $Nu\ h^*/k^*$. In addition, the time required to obtain the solution for a special case is much longer than for the one-dimensional solution. Only one example was therefore calculated; namely, the temperature distribution within the walls of a heat exchanger composed of rectangular passages, as shown in figure 9. The ratio of the two side lengths of the rectangle is 1 to 5. The ratio of the hydraulic diameter to the short side of this passage is 1.67 and the dimensionless wall thickness is 0.6. Figure 17 presents the results of the calculation using the relaxation method with a network of 88 points. Lines of constant temperature (isotherms) are shown within the portion of the heat-exchanger walls that is shaded in figure 9. As may be seen, the heat flow within this wall is mainly in the direction normal to the wall surfaces. The maximum temperature differences on any normal to the surface are not very different from the value in a flat plate as calculated in equation (42). The temperature differences along the surface of the wall are

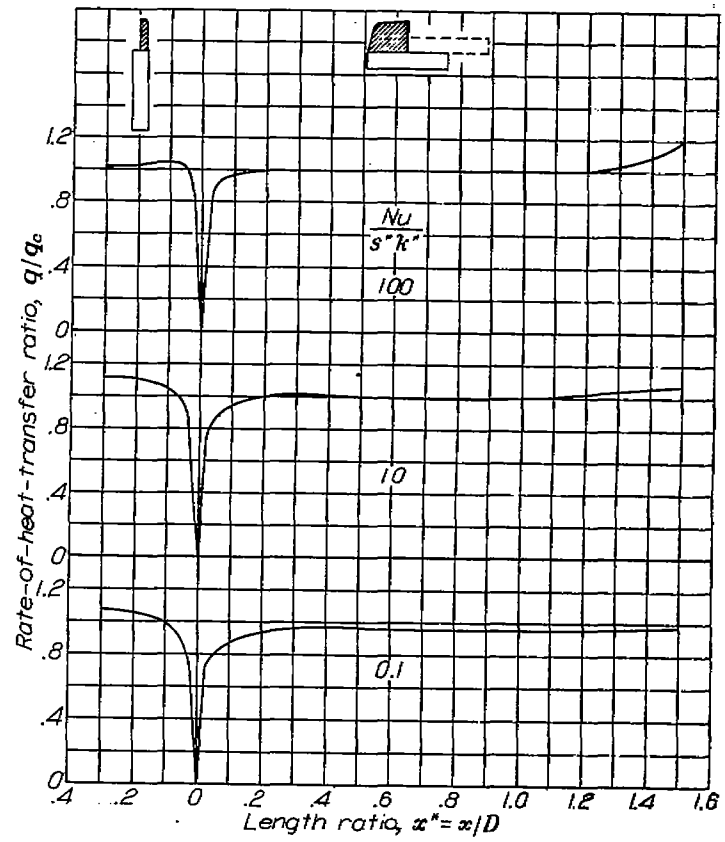


FIGURE 16.—Local rate of heat transfer from passage of thin-walled rectangular heat exchanger (fig. 10).

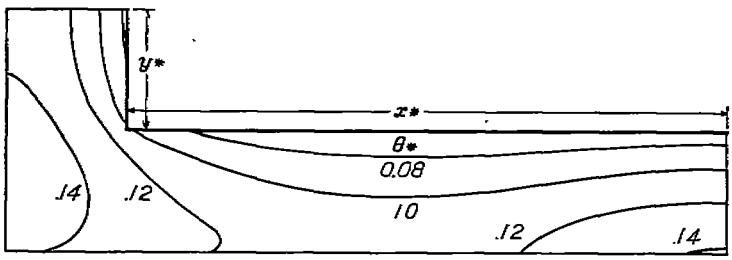


FIGURE 17.—Isotherms in internally heated walls of thick-walled rectangular heat exchanger. (Shaded portion of fig. 9 shown.) $Nu/s^*k^*$, 10.0; ratio of flow area to toal area, 0.416; $s^*$, 0.6; $y^*/x^*$, 1/5.

appreciably smaller than the temperature differences across the wall. The values of the one-dimensional solution cannot therefore be expected to apply to this case. Actually, the temperature difference found in figure 17 along the surface of the wall is considerably greater than for the corresponding one-dimensional case. In addition, heat is generated within the corner area of the rectangular-wall configuration and has to be conducted away along comparatively long paths. An additional temperature increase can therefore be found within this corner area.

## CONCLUSIONS

A method to calculate the temperature distribution in a heat exchanger composed of noncircular flow passages with internally heated walls has been presented.

Local heat-transfer coefficients along the circumference of the heat-exchanger passages were obtained from flow measurements made by Nikuradse, assuming similarity between the velocity and temperature fields. The heat-transfer coefficients, as determined in this manner, decrease sharply near the corners of the passages and vanish at the corners. This decrease becomes more pronounced as the corner angle is increased. Near the corners these coefficients are essentially influenced only by the magnitude of the included angle of the corner.

It was shown that the dimensionless temperature distribution within the passage walls depends on a single parameter, provided the dimensionless wall thickness is small. Numerical evaluations for triangular- and rectangular-passage configurations for a wide range of the aforementioned parameter were carried out. The results of these evaluations are presented so that temperature differences arising in the walls of heat exchangers with the investigated passage shapes for any condition within the range of practical interest can be read off one of several curves. These curves show a temperature increase near the corners of the passages. This increase becomes more pronounced for high Nusselt numbers based on the average heat-transfer coefficient, for low wall-thickness ratios, and for low ratios of the conductivity of the wall to the conductivity of the coolant.

The dimensionless temperature distribution for thick-walled heat exchangers depends on the wall-thickness ratio in addition to the property parameter. Because the time required to calculate temperature distributions in the whole field of interest determined by the two parameters is prohibitive, only a specific example was evaluated numerically. The method of calculation is presented in great detail, however, so that evaluations for other interesting cases can be carried out.

LEWIS FLIGHT PROPULSION LABORATORY
NATIONAL ADVISORY COMMITTEE FOR AERONAUTICS
CLEVELAND, OHIO, *October 4, 1950*

# APPENDIX

## SOLUTION BY RUNGE-KUTTA METHOD

Equation (16) is of the following form:

$$\frac{d^2\theta^*}{dx^{*2}} - f(x^*)\,\theta^* + 1 = 0 \tag{A1}$$

The boundary conditions are

$$\left.\begin{aligned}\left(\frac{d\theta^*}{dx^*}\right)_{x^*=a} &= 0\\ \left(\frac{d\theta^*}{dx^*}\right)_{x^*=b} &= 0\end{aligned}\right\} \tag{A2}$$

where $a$ and $b$ are points of symmetry.

In general, a solution of equation (A1) could be obtained by assuming an initial value of $\theta^*$ at point $a$ in addition to the first of the boundary conditions (A2) and by working the solution toward point $b$ using a numerical method of integration. If the boundary condition at point $b$ is not satisfied, the solution has to be repeated with a new initial value. This trial-and-error process is tedious and can be avoided by splitting equation (A1) in such a manner as to keep an undetermined constant $c$ in the solution. This constant is finally determined by satisfying the second boundary condition. Let

$$\theta^* = \theta_1^* + c\theta_2^* \tag{A3}$$

$$\frac{d^2\theta_1^*}{dx^{*2}} - f(x^*)\,\theta_1^* + 1 = 0$$

$$\frac{d^2\theta_2^*}{dx^{*2}} - f(x^*)\,\theta_2^* = 0$$

where

$$\theta_1^*(a) = 0 \qquad \theta_2^*(a) = 1$$

$$\left(\frac{d\theta_1^*}{dx^*}\right)_a = 0 \qquad \left(\frac{d\theta_2^*}{dx^*}\right)_a = 0$$

These expressions still satisfy equation (A1) and the first of the boundary conditions (A2). After the solutions for $\theta_1^*$ and $\theta_2^*$ have been numerically obtained, the constant $c$ is determined so that the boundary condition at point $b$ is fulfilled; thus

$$\left(\frac{d\theta_1^*}{dx^*}\right)_b + c\left(\frac{d\theta_2^*}{dx^*}\right)_b = 0$$

or

$$c = -\frac{\left(\frac{d\theta_1^*}{dx^*}\right)_b}{\left(\frac{d\theta_2^*}{dx^*}\right)_b}$$

The final temperature distribution is given by equation (A3).

The temperature distribution in a thin-walled heat exchanger with triangular passages was calculated in this manner (for $Nu/s^*k^*=10$) and was compared with the corresponding curve in figure 13. The Runge-Kutta method (reference 10) was used for the numerical integration. This particular comparison showed differences of 2.2 percent of the temperature ratio near the corners of the passages and smaller deviations elsewhere. The temperature curves are uncertain to the same order of magnitude, however, because of the freedom in the extrapolation of the heat-transfer-coefficient curves. The simpler relaxation method is therefore regarded satisfactory for the present purpose.

## REFERENCES


1. McAdams, William H.: Heat Transmission. McGraw-Hill Book Co., Inc., 2d ed., 1942.
2. Jakob, Max: Heat Transfer. John Wiley & Sons, Inc., 1949.
3. Nikuradse, J.: Untersuchungen über turbulente Strömungen in nicht kreisförmigen Rohren. Ingenieur-Archiv, Bd. 1, 1930, S. 306–332.
4. Nikuradse, J.: Geschwindigkeitsverteilung in turbulenten Strömungen. VDI Zeitschr., Bd. 70, Nr. 37, Sept. 11, 1926, S. 1229–1230.
5. Prandtl, L.: Turbulent Flow. NACA TM 435, 1927.
6. Kalikhman, L. E.: Heat Transmission in the Boundary Layer. NACA TM 1229, 1949.
7. Latzko, H.: Heat Transfer in a Turbulent Liquid or Gas Stream. NACA TM 1068, 1944.
8. Eckert, E. R. G.: Introduction to the Transfer of Heat and Mass. McGraw-Hill Book Co., Inc., 1950, pp. 128–140.
9. Emmons, H. W.: The Numerical Solution of Heat-Conduction Problems. Trans. A.S.M.E., vol. 65, no. 6, Aug. 1943, pp. 607–612.
10. Scarborough, James B.: Numerical Mathematical Analysis. Johns Hopkins Press (Baltimore), 1930.